

Autoregressive Modeling for Fading Channel Simulation

Kareem E. Baddour, *Student Member, IEEE*, and Norman C. Beaulieu, *Fellow, IEEE*

Abstract—Autoregressive stochastic models for the computer simulation of correlated Rayleigh fading processes are investigated. The unavoidable numerical difficulties inherent in this method are elucidated and a simple heuristic approach is adopted to enable the synthesis of accurately correlated, bandlimited Rayleigh variates. Startup procedures are presented, which allow autoregressive simulators to produce stationary channel gain samples from the first output sample. Performance comparisons are then made with popular fading generation techniques to demonstrate the merits of the approach. The general applicability of the method is demonstrated by examples involving the accurate synthesis of nonisotropic fading channel models.

Index Terms—Autoregressive processes, bandlimited stochastic processes, multipath channels, nonisotropic scattering, Rayleigh channels, simulation.

I. INTRODUCTION

THE bandlimited Rayleigh fading process, whose power spectral density (PSD) is zero past the maximum Doppler frequency, appears in many physical models of mobile radio channels. Its emulation has been of theoretical and practical interest to the wireless community for many years, as the design and optimization of modern communication systems cannot be carried out without computer simulations. The classical fading simulator application is to generate a single sequence of correlated Rayleigh variates in accordance with Clarke's wide-sense stationary (WSS) isotropic scattering model [1]. However, the scattering encountered in many environments is nonisotropic, which strongly affects the second-order statistics of the channel. A desirable simulator feature is the ability to emulate such directional fading scenarios, for which the real and imaginary Gaussian sequences underlying the sampled Rayleigh channel can exhibit cross-correlations. This paper addresses the development of a simulation methodology, which

can be easily used to accurately synthesize such generalized flat Rayleigh fading channels.

In the communications literature, a number of different algorithms have been proposed for the generation of correlated Rayleigh random variates (e.g., [2]–[5]). Among these, simulators based on either a sum-of-sinusoids approach, on a white noise filtering method, or on the inverse discrete Fourier transform (IDFT) algorithm have become popular. Recently, significant problems were found to exist with the stochastic behavior of commonly used sum-of-sinusoids designs. In particular, it was shown in [6] that the classical Jakes' simulator produces fading signals that are not WSS. Careful redesigns of the sum-of-sinusoids models, such as those proposed in [7] and [8], are required to remove the stationarity problem while maintaining the accuracy of the correlation statistics. The IDFT technique, on the other hand, is well known to be a high-quality and efficient fading generator [2]. Unfortunately, a disadvantage of the IDFT method is that all samples are generated with a single fast Fourier transform (FFT) operation. The storage requirements of this approach can make it unattractive for the generation of a very large number of variates. The search for a fading simulator that can produce statistically accurate variates "as they are needed" also motivates our work herein.

In this paper, we consider the use of a general autoregressive (AR) modeling approach for the accurate generation of correlated Rayleigh processes. Essentially, this technique employs all-pole infinite-impulse response (IIR) filtering to shape the spectrum of uncorrelated Gaussian variates. Unlike previous white noise filtering methods, precise matching of the theoretical statistics is possible over the order of the model for practical finite-length implementations. Furthermore, the model parameters are easily computed. Previously, AR models have been used with success to predict fading channel dynamics for the purposes of Kalman-filter-based channel estimation (e.g., [9]–[12]) and for long-range channel prediction [13]. They have also been used by several authors to simulate correlated Rayleigh fading [10], [14], though in [10] and [14], low-order AR processes were adopted, which do not provide a good match to the desired bandlimited correlation statistics. In [15], the authors also attempted to use an AR fading generator, but ran into stability problems and abandoned this approach.

In this paper, we examine AR fading simulators in detail. First, we demonstrate that it is the highly deterministic nature of narrowband Doppler fading processes that leads to the numerical problems faced by the AR method in this application. A simple heuristic approach is proposed to enable the

Manuscript received April 24, 2003; revised October 24, 2003; accepted May 4, 2004. The editor coordinating the review of this paper and approving it for publication is C. Xiao. This work was supported by a postgraduate scholarship from the Natural Sciences and Engineering Research Council of Canada (NSERC), by an Industry Canada Fessenden Postgraduate Scholarship, by an Ontario Graduate Scholarship in Science and Technology, and by the Alberta Informatics Circle of Research Excellence (iCORE). This paper was presented in part at the 2001 Global Telecommunications Conference (GLOBECOM '01), San Antonio, TX, November 2001.

K. E. Baddour is with the Department of Electrical and Computer Engineering, Queen's University, Kingston, ON K7L 3N6, Canada (e-mail: baddourk@ee.queensu.ca).

N. C. Beaulieu is with the Department of Electrical and Computer Engineering, University of Alberta, Edmonton, AB T6G 2V4, Canada (e-mail: beaulieu@ee.ualberta.ca).

Digital Object Identifier 10.1109/TWC.2005.850327

synthesis of accurately correlated bandlimited Rayleigh variates. Startup procedures are described, which allow AR generators to produce stationary and statistically correct Rayleigh variates from the first output sample. Performance comparisons are then made with popular Rayleigh fading generators to demonstrate the merits of the AR method. The accurate synthesis of nonisotropic Rayleigh fading models is also demonstrated. To the best of our knowledge, no complete study of using an AR approach to accurately generate bandlimited Rayleigh random processes has been reported in the literature.

The remainder of this paper is organized as follows. Section II briefly reviews correlated Rayleigh fading models and popular variate generation techniques. Section III describes the AR method of generating stationary bandlimited Rayleigh processes. Section IV compares the method to both the IDFT and a WSS sum-of-sinusoids simulator. The ability of the AR generator to accurately simulate nonisotropic models is also demonstrated. Section V concludes the paper.

II. FADING SIMULATION

A. Correlated Fading Models

A Rayleigh characterization of the land mobile radio channel follows from the Gaussian WSS uncorrelated scattering fading model [16], where the fading process is modeled as a complex Gaussian process. In this model, the variability of the wireless channel over time is reflected in its autocorrelation function (ACF). This second-order statistic generally depends on the propagation geometry, the velocity of the mobile, and the antenna characteristics. A common assumption is that the propagation path consists of a two-dimensional isotropic scattering with a vertical monopole antenna at the receiver [17]. In this case, the theoretical PSD associated with either the in-phase or quadrature portion of the received fading signal has the well-known U-shaped bandlimited form [17]

$$S(f) = \begin{cases} \frac{1}{\pi f_d \sqrt{1 - (\frac{f}{f_d})^2}}, & |f| \leq f_d \\ 0, & \text{elsewhere} \end{cases} \quad (1)$$

where f_d is the maximum Doppler frequency in Hertz, given by $f_d = v/\lambda$, v is the mobile speed and λ is the wavelength of the received carrier wave. The corresponding normalized (unit variance) continuous-time autocorrelation of the received signal under these conditions is $R(\tau) = J_0(2\pi f_d \tau)$, where $J_0(\cdot)$ is the zeroth-order Bessel function of the first kind [17]. For the purposes of discrete-time simulation of this model, ideally generated in-phase and quadrature Gaussian processes should each have the autocorrelation sequence

$$R[n] = J_0(2\pi f_m |n|) \quad (2)$$

where $f_m = f_d T$ is the maximum Doppler frequency normalized by the sampling rate $1/T$. Furthermore, in this model the

in-phase and quadrature processes must be independent and each must have zero mean for Rayleigh fading.

Variations on the PSD in (1) have been proposed based on more complicated propagation models. A PSD derived without assuming that the incoming waves are only horizontal in three-dimensional space is given in [18]. This bandlimited PSD is very similar to (1), but does not have asymptotes approaching infinity at the band edges of the fading spectrum. Improvements to this spectrum have been proposed in [19]. A three-dimensional model with isotropic scattering in all three directions is examined in [20]. In this model, the PSD has flat bandlimited characteristics with a normalized ACF

$$R[n] = \text{sinc}(2f_m |n|) \quad (3)$$

where $\text{sinc}(x) = \sin(\pi x)/\pi x$. Complex Gaussian fading models have also been proposed for nonisotropic scattering scenarios (e.g., [21], [22]). In such environments, the Doppler PSD is not necessarily even symmetric, which results in a channel ACF that has an imaginary component. As a result, the underlying real in-phase and quadrature fading processes experience cross-correlations. In general, the theoretical Doppler power spectrum is bandlimited, since the maximum Doppler shift is a finite quantity that is proportional to the mobile velocity. Thus, the focus in this paper is on the accurate synthesis of complex Gaussian processes with a specified bandlimited spectrum.

B. Correlated Variate Generation

Exact generation of N Gaussian variates with an arbitrary correlation can be achieved in principle by decomposing the desired $N \times N$ covariance matrix $\mathbf{R} = \mathbf{G}\mathbf{G}^H$, where \mathbf{G}^H denotes the Hermitian transpose of \mathbf{G} , then multiplying N independent Gaussian variates by \mathbf{G} [23, pp. 254–256]. The Cholesky factorization, which can be performed with $O(N^2)$ operations for Toeplitz matrices, is an efficient choice for this decomposition. For bandlimited processes, however, an approximation using a singular value decomposition is typically required due to numerical problems arising from an ill-conditioned covariance matrix. In this case factorization requires $O(N^3)$ operations, which restricts applicability of the method to the generation of very small sample sizes.

A popular method for modeling the Rayleigh flat fading channel is to sum the outputs from N_s complex sinusoidal generators [17]. In practice, the generated sequence closely approximates a complex Gaussian process provided a sufficient number of sinusoids are used. With proper choice of the distribution of the sinusoid frequencies (see, e.g., [6]), the process autocorrelation approaches that represented by (2) as $N_s \rightarrow \infty$.

Correlated Rayleigh variates can also be generated by filtering two zero-mean independent white Gaussian processes and then adding the outputs in quadrature. Here, rational transfer function approximations of the nonrational PSD in (1) are typically used to shape the spectrum. The autocorrelation

properties of the generated sequences are determined by the choice of filter. Many possibilities for this choice exist (e.g., [3], [5], [15]). In general, these approaches do not provide precise matching of the theoretical statistics.

Another popular technique for generating correlated Rayleigh variates is Smith's IDFT algorithm [24]. Here, the IDFT operation is applied to sequences of uncorrelated complex Gaussian variates, each sequence weighted by appropriate filter coefficients to shape the PSD. Young and Beaulieu [2] modified Smith's algorithm for greater computational efficiency and provided a statistical analysis of the method. By considering the quality of the generated variates and the computational effort, a comparison of the IDFT generator with the sum-of-sinusoids technique and a finite-impulse response (FIR) filter method concluded that the IDFT generator is superior [2].

III. AR MODELING OF BANDLIMITED RAYLEIGH RANDOM PROCESSES

A. Model Computation

Autoregressive models are commonly used to approximate discrete-time random processes [25]. This is due to the simplicity with which their parameters can be computed and due to their correlation matching property. A complex AR process of order p [AR(p)] can be generated via the time domain recursion

$$x[n] = -\sum_{k=1}^p a_k x[n-k] + w[n] \quad (4)$$

where $w[n]$ is a complex white Gaussian noise process with uncorrelated real and imaginary components. For Rayleigh variate generation, $w[n]$ has zero mean and the simulator output is $|x[n]|$. The AR model parameters consist of the filter coefficients $\{a_1, a_2, \dots, a_p\}$ and the variance σ_p^2 of the driving noise process $w[n]$. The corresponding PSD of the AR(p) process has the rational form [25]

$$S_{xx}(f) = \frac{\sigma_p^2}{\left|1 + \sum_{k=1}^p a_k \exp(-j2\pi f k)\right|^2}. \quad (5)$$

Although the Doppler spectrum models proposed for mobile radio are not rational, an arbitrary spectrum can be closely approximated by an AR model of sufficiently large order. The basic relationship between the desired model ACF $R_{xx}[k]$ and the AR(p) parameters is given by [25]

$$R_{xx}[k] = \begin{cases} -\sum_{m=1}^p a_m R_{xx}[k-m], & k \geq 1 \\ -\sum_{m=1}^p a_m R_{xx}[-m] + \sigma_p^2, & k = 0. \end{cases} \quad (6)$$

In matrix form this becomes for $k = 1, 2, \dots, p$

$$\mathbf{R}_{xx} \mathbf{a} = -\mathbf{v} \quad (7a)$$

where

$$\mathbf{R}_{xx} = \begin{bmatrix} R_{xx}[0] & R_{xx}[-1] & \cdots & R_{xx}[-p+1] \\ R_{xx}[1] & R_{xx}[0] & \cdots & R_{xx}[-p+2] \\ \vdots & \vdots & \ddots & \vdots \\ R_{xx}[p-1] & R_{xx}[p-2] & \cdots & R_{xx}[0] \end{bmatrix}$$

$$\mathbf{a} = [a_1 \ a_2 \ \cdots \ a_p]^T$$

$$\mathbf{v} = [R_{xx}[1] \ R_{xx}[2] \ \cdots \ R_{xx}[p]]^T \quad (7b)$$

and

$$\sigma_p^2 = R_{xx}[0] + \sum_{k=1}^p a_k R_{xx}[-k]. \quad (8)$$

Given the desired ACF sequence, the AR filter coefficients can thus be determined by solving the set of p Yule-Walker equations in (7a). These equations can in principle be solved efficiently by the Levinson-Durbin recursion in $O(p^2)$. Since \mathbf{R}_{xx} is an autocorrelation matrix, it is positive semidefinite and can be shown to be singular only if the process is purely harmonic and consists of $p-1$ or fewer sinusoids [27]. In all other cases, the inverse \mathbf{R}_{xx}^{-1} exists and the Yule-Walker equations are guaranteed to have the unique solution $\mathbf{a} = -\mathbf{R}_{xx}^{-1} \mathbf{v}$. The generated AR(p) process has the ACF [25]

$$\hat{R}_{xx}[k] = \begin{cases} R_{xx}[k], & 0 \leq k \leq p \\ -\sum_{m=1}^p a_m \hat{R}_{xx}[k-m], & k > p. \end{cases} \quad (9)$$

That is, the simulated process has the attractive property that its sampled ACF perfectly matches the desired sampled ACF up to lag p . The remaining ACF extension is characterized by the property that the generated time series is the most random one (maximum entropy) which has the assigned first $p+1$ ACF lags [25].

B. Ill Conditioning of the Yule-Walker Equations

In solving the Yule-Walker equations, the condition of the autocorrelation matrix is an important consideration in determining the accuracy of the solution. A measure of the ill conditioning is provided by the white noise variance parameter σ_p^2 . Moreover, it can be shown that [26, p. 354]

$$|\mathbf{R}_{xx}| = \prod_{m=0}^{p-1} \sigma_m^2 \quad (10)$$

where $|\mathbf{R}_{xx}|$ denotes the determinant of \mathbf{R}_{xx} and σ_m^2 represents the driving white noise variance corresponding to an AR(m) model of the process. Consequently, if the values of the σ_m^2 are very small, \mathbf{R}_{xx} is nearly singular so that significant errors in the computed parameters are expected and unavoidable, regardless of the method used to solve (7a). In these cases,

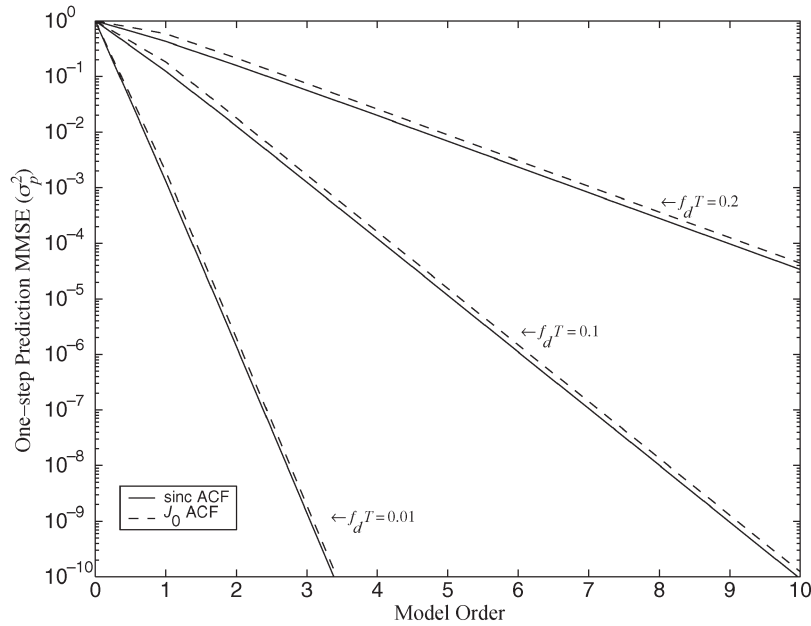


Fig. 1. The one-step prediction MMSE for the Bessel ACF and sinc ACF versus the model order.

numerical problems in the solution typically yield unstable model filters.

To investigate the stability and accuracy of AR models of bandlimited processes, in the sequel we consider the behavior of σ_p^2 with increasing AR order. To begin, it is useful to note that σ_p^2 in the AR formulation is equivalent to the minimum mean square error (MMSE) of a one-step-ahead linear predictor of order p for the bandlimited process being modeled [27]. A lower bound on the MMSE is known from prediction theory to be given by the infinite prediction memory case, in which case the asymptotic σ_p^2 can be expressed via the Kolmogoroff–Szegö formula [28, p. 491]

$$\lim_{p \rightarrow \infty} \sigma_p^2 = \exp \left[\frac{1}{2\pi} \int_{-\pi}^{\pi} \ln S_{xx}(e^{j\omega}) d\omega \right] \quad (11)$$

where $\omega = 2\pi f$, and $S_{xx}(e^{j\omega}) = \sum_{k=-\infty}^{\infty} R_{xx}[k]e^{-jk\omega}$ is the desired power spectrum of the process. From (11), we find that a stochastic process whose spectrum is zero over some finite frequency domain has a zero asymptotic prediction error. Such a process is said to be *deterministic* since its future can in principle be predicted exactly in a mean-square sense from knowledge of all its past samples taken greater than the Nyquist rate [29]. This implies that the rapid time variation of a complex Gaussian fading channel process, which is due to bandlimited Doppler spreading, is in theory deterministic.¹

A more important consideration for our stability investigation is how fast σ_p^2 converges to its zero asymptotic

value. In [32], a study of the behavior of linear prediction errors as the predictor order increases was performed. The MMSE of one-step-ahead linear prediction was observed to decrease *exponentially* to zero with increasing predictor order for many processes with bandlimited spectra. The authors in [32] conjectured that this rapid decay occurs for all bandlimited processes. In the signal processing literature, the exponential decay of the prediction error has been theoretically proven only for flat bandlimited spectra (sinc autocorrelation) in [33]. Although it does not appear to be well known, a more general proof of this result for any real bandlimited process can be found in the mathematical literature in [34]. More precisely, it can be shown in this case that for large p and bandlimit f_d , the MMSE of the one-step-ahead linear prediction vanishes as [34]

$$\sigma_p^2 \sim k [\sin(\pi f_d T)]^{2p} \quad (12)$$

when the sampling rate $1/T$ is greater than the Nyquist rate $2f_d$ and where k is a constant. With the exception of a different constant term k , we have verified that this asymptotic rate of decay of σ_p^2 holds for the bandlimited processes of interest in mobile radio. For example, in Fig. 1, σ_p^2 is plotted versus the model order for various values of $f_d T$ assuming that the random process has the ACFs in (2) and (3). The exponential asymptotic rate of decay of σ_p^2 is only a function of the normalized Doppler bandlimit and not of the actual process spectrum. Furthermore, since f_d is typically several orders of magnitude smaller than the sampling rate, it can be seen that σ_p^2 achieves its asymptotic rate of decay beginning at small AR orders and that this rate is very rapid. Thus, for narrowband Doppler processes, severely ill-conditioned Yule–Walker equations are unavoidable for all but very small AR model orders p . In light of this fact, and since the lower

¹This paper focuses on discrete-time bandlimited processes. Related recent work, which considers the predictability of continuous-time bandlimited fading processes, can be found in [30] and [31].

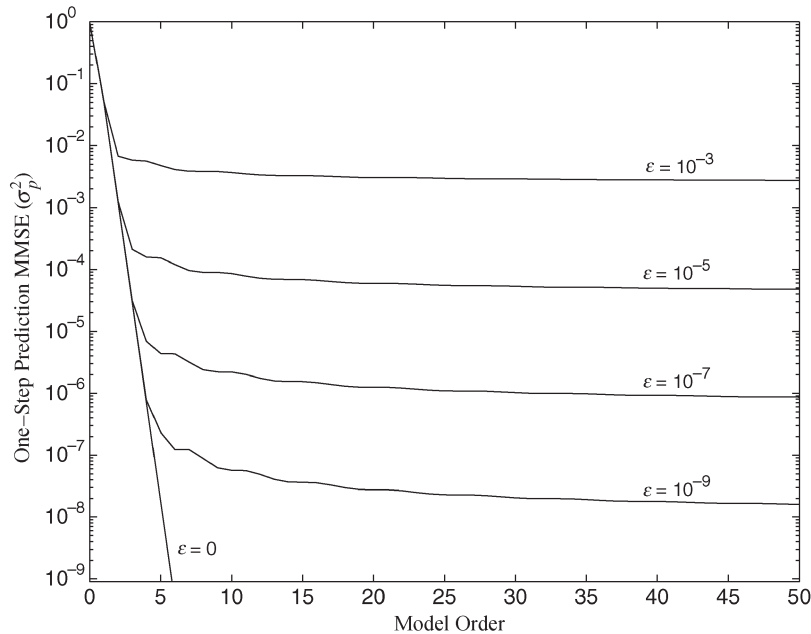


Fig. 2. The one-step prediction MMSE for the Bessel ACF versus the model order for various ϵ when $f_m = 0.05$.

order models result in a poor match to the desired band-limited ACF, it is not surprising that previous investigations (e.g., [15]) concluded that an AR parameterization cannot accurately model the $J_0(\cdot)$ autocorrelation sequence. In the sequel we overcome the numerical problems, making accurate AR simulation viable, including the difficult $J_0(\cdot)$ autocorrelation sequence.

From the preceding discussion, it does not seem possible to generate stable AR filters of large orders using finite word-length computations to accurately model bandlimited spectra. However, a simple heuristic approach that can be used to resolve the numerical problems is to improve the conditioning of the autocorrelation matrix \mathbf{R}_{xx} by increasing the values along its principal diagonal by a very small positive amount ϵ . This is equivalent, of course, to adding white noise of variance ϵ to the original process. The addition of this spectral bias removes the bandlimitation of the original spectrum and creates a nondeterministic or *regular* process that in some sense closely approximates the original process. As a result, σ_p^2 no longer decays exponentially to zero with increasing model order p . In Fig. 2, σ_p^2 is plotted versus the model order for various values of ϵ assuming that the random process has the Bessel autocorrelation in (2). Similar curves result for other bandlimited spectra [35]. We observe from Fig. 2 that while σ_p^2 monotonically decreases with p , it now approaches a lower bound

$$\lim_{p \rightarrow \infty} \sigma_p^2 = \exp \left\{ \frac{1}{2\pi} \int_{-\pi}^{\pi} \ln [S_{xx}(e^{j\omega}) + \epsilon] d\omega \right\} > 0 \quad (13)$$

for asymptotically large p . The inequality in (13) follows since $S_{xx}(e^{j\omega}) \geq 0$. The choice of ϵ represents a tradeoff between

the improved condition number of \mathbf{R}_{xx} and the bias introduced in the model. By choosing ϵ appropriately, the lower bound on σ_p^2 can be made large enough to enable the stable computation of a large-order AR model. The first $p + 1$ autocorrelation lags of the resulting AR(p) process will then be

$$\hat{R}_{xx}[m] = \begin{cases} R_{xx}[0] + \epsilon, & m = 0 \\ R_{xx}[m], & m = 1, 2, \dots, p. \end{cases} \quad (14)$$

That is, while the zeroth autocorrelation lag will contain a small additive error, the next p lags will match those of the desired theoretical ACF.

We note that the heuristic addition of a white noise component to overcome ill conditioning was recently used in [14]. However, a proper justification for the inclusion of the bias ϵ was not provided. The singularity at the band edge of the PSD in (1) is not the sole cause of the numerical problems, as suggested in [14]. Moreover, the “stiffness” of the autocorrelation matrix is manifested for any bandlimited PSD shape and it is the deterministic nature of bandlimited processes that is the main cause of the numerical problems experienced in these cases.

C. Stationary Generation

The AR generator, like other rational transfer function approximation methods, produces correlated variates by filtering white Gaussian noise sources. The common practice of passing white noise through a fixed filter produces transients due to nonstationary initial conditions. Theory dictates that for a stationary output to be strictly achieved, the filter must have had an input of white noise for all of $n \geq -\infty$ [36]. In practice, it is necessary to run the filter for a while before the transient effects become negligible and for the output to

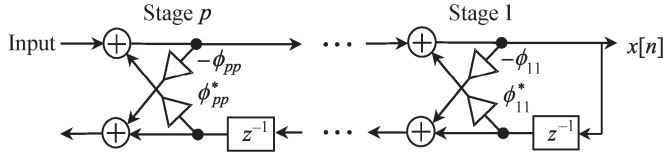


Fig. 3. The all-pole lattice representation of the AR filter.

achieve asymptotic stationarity [27]. In the sequel, we briefly describe two startup procedures that allow the AR generator to produce stationary variates from the first output sample. Both methods use a time-varying IIR filter to generate the first p stationary outputs with the correct correlation values, where p is the desired model order. This provides the appropriate initial conditions for the fixed p th order AR filter to subsequently generate a sequence which is truly stationary. Such a startup procedure is particularly useful when a large AR order is chosen to provide accurate correlation matching, as in these cases, a large number of variates must typically be discarded before the transient effects decay.

The first start-up technique appears implicitly in a method for synthesizing fractional Gaussian noise [37]. The procedure uses the result that for a zero-mean stationary Gaussian process, the conditional mean and variance of $x[k]$, given the past values $x[k - 1], x[k - 2], \dots, x[0]$ may be written as [38]

$$\begin{aligned}
 m_k &= E \{x[k] | x[k - 1], x[k - 2], \dots, x[0]\} \\
 &= - \sum_{j=1}^k \phi_{kj} x[k - j] \tag{15}
 \end{aligned}$$

$$\begin{aligned}
 v_k &= \text{Var} \{x[k] | x[k - 1], x[k - 2], \dots, x[0]\} \\
 &= R_{xx}[0] \prod_{j=1}^k (1 - |\phi_{jj}|^2). \tag{16}
 \end{aligned}$$

Here, ϕ_{jj} denotes the j th reflection coefficient [25] of $\{x[k]\}$ and the ϕ_{kj} are the AR coefficients for a k th order model. For a particular k , the ϕ_{kj} coefficients for $j = 1, 2, \dots, k$ can be computed by an $O(k^2)$ Levinson–Durbin execution. Note that the variance v_k in (16) is equal to the variance σ_k^2 of the driving noise in the context of a k th order AR process. The start-up procedure for generating the first p stationary correlated complex Gaussian variates is then as follows.

- 1) Generate a starting value $x[0]$, whose in-phase and quadrature components are drawn independently from a Gaussian distribution $N(0, R_{xx}[0])$. Set $v_0 = R_{xx}[0]$.
- 2) For $k = 1, \dots, p - 1$, calculate the ϕ_{kj} coefficients for $j = 1, 2, \dots, k$ using the Levinson recursion. Compute $m_k = - \sum_{j=1}^k \phi_{kj} x[k - j]$ and $v_k = (1 - |\phi_{kk}|^2)v_{k-1}$. Generate the next variate $x[k]$, whose in-phase and quadrature components are drawn independently from $N(m_k, v_k)$.

TABLE I
ORDER OF ϵ OBSERVED TO YIELD THE MOST ACCURATELY CORRELATED AR SIMULATOR OUTPUTS FOR THE $J_0(\cdot)$ ACF MODEL

f_m	ϵ
0.001	10^{-5}
0.005	10^{-6}
0.01	10^{-7}
0.05	10^{-8}

The remainder of the stationary sequence can then be generated using the fixed p th order AR filter as per (4). While this procedure requires solving for the AR coefficient parameter set of all orders less than and including the desired AR order p , these parameters can be obtained at the intermediate steps of a single Levinson–Durbin execution.

An alternative start-up method can be achieved by using a time-varying lattice filter [39] implementation of the p th order AR filter. Here the optimum lattice filter coefficients are given by the reflection coefficients $\phi_{jj}, j = 1, \dots, p$. Since the reflection coefficients of the lower order do not change as the AR model order is increased [28], only one set of parameters is required. The all-pole lattice representation of the AR filter is shown in Fig. 3. The start-up procedure consists of switching on one stage of the lattice form at a time, with the real and imaginary components of the complex Gaussian white noise input at iteration $k = 0, 1, \dots, p - 1$ chosen independently from a Gaussian distribution $N(0, v_k)$, where $v_0 = R_{xx}[0]$ and $v_k = (1 - |\phi_{kk}|^2)v_{k-1}$. The signals in all modules greater than the time index k should have zero value until that stage is switched on.

IV. PERFORMANCE EVALUATION

In this section, we evaluate the suitability of the AR generator for producing high-quality bandlimited Rayleigh variates. Comparisons are made to a WSS sum-of-sinusoids simulator and to the IDFT technique, which was demonstrated in [2] to be the most efficient and highest quality method among several popular correlated Rayleigh variate generators. The quantitative measures that are used for this comparison are described first.

A. Quantitative Measures

Quantitative quality measures for generated random variates that are in a form familiar to communication engineers have been proposed in [40]. The proposed measures represent approximately the difference in signal-to-noise ratio in decibels predicted to meet a specified performance (error rate, outage, etc.) when an imperfect sequence of random variates is used during simulation rather than a statistically “ideal” sequence. See [40] for more details. Two quality measures have been defined in [40] as follows. The first measure, called the *mean basis power margin*, is given by

$$\mathcal{G}_{\text{mean}} = \frac{1}{\sigma_x^2 L} \text{trace} \{ \mathbf{C}_x \mathbf{C}_x^{-1} \mathbf{C}_x \} \tag{17}$$

TABLE II
A COMPARISON OF THE AR, IDFT, AND SUM-OF-SINUSOIDS METHODS
OF GENERATING BANDLIMITED RAYLEIGH VARIATES FOR
COVARIANCE SEQUENCE LENGTH 200

		$\mathcal{G}_{\text{mean}}$	\mathcal{G}_{max}
IDFT Method	(T)	0.00076 dB	0.00081 dB
	(E)	0.0034 dB	0.0037 dB
AR Filtering	AR(20) (T)	2.7 dB	2.9 dB
	AR(20) (E)	2.6 dB	2.9 dB
	AR(50) (T)	0.29 dB	0.43 dB
	AR(50) (E)	0.26 dB	0.40 dB
	AR(100) (T)	0.13 dB	0.28 dB
	AR(100) (E)	0.11 dB	0.26 dB
	AR(200) (T)	0 dB	0 dB
	AR(200) (E)	0.00074 dB	0.00078 dB
Sum of Sinusoids	8 sinusoids (E)	38.8 dB	41.8 dB
	16 sinusoids (E)	3.5 dB	4.9 dB
	64 sinusoids (E)	0.0074 dB	0.0080 dB
	128 sinusoids (E)	0.0020 dB	0.0022 dB

and the second, the *maximum basis power margin*, is defined as

$$\mathcal{G}_{\text{max}} = \frac{1}{\sigma_{\mathbf{x}}^2} \max\{\text{diag}\{\mathbf{C}_{\mathbf{x}}\mathbf{C}_{\mathbf{x}}^{-1}\mathbf{C}_{\mathbf{x}}\}\}. \quad (18)$$

In (17) and (18), $\sigma_{\mathbf{x}}^2$ is the variance of the reference (ideal) distribution, $\mathbf{C}_{\mathbf{x}}$ is the $L \times L$ covariance matrix of any length- L subset of adjacent variates produced by the stationary random variate generator, and $\mathbf{C}_{\mathbf{x}}$ represents the desired covariance matrix of L ideally distributed variates. For some variate generation schemes, $\mathbf{C}_{\mathbf{x}}$ can be determined directly. For the AR variate generation method, this is easily accomplished using (9) and (14). Alternatively, empirical techniques can be used to estimate this matrix from the generator output.

B. Tested Simulation Methods

1) *AR Method*: The method used was that of Section III. Based on our numerical work, the value of the bias ϵ that yields the most accurate AR model computation was observed to depend mainly on the Doppler rate. Table I lists the order of the constant ϵ that was empirically found to minimize (17) and (18) for the $J_0(\cdot)$ ACF using MATLAB on a Pentium IV machine. The numerical conditioning of the Yule-Walker equations is worse for smaller Doppler bandwidths, which necessitates a larger ϵ . The dependence of the choice of ϵ on the AR model order is not significant for typical filter lengths. The values in Table I are recommended for model orders up to 1000. If the AR order is much greater, then a small increase in the ϵ values in Table II provides an improvement to the simulator accuracy.

Our AR implementation used the lattice start-up procedure of Section III to generate the first p stationary variates. Since direct IIR filtering requires fewer computations than lattice filtering, the remainder of the variates were generated by a direct structure using the MATLAB function `filter`. The appropriate initial conditions for this filter, corresponding to the first p generated stationary variates, were set using the MATLAB function `filtic`.

2) *IDFT Method*: The simulator used was implemented as described in [2]. The MATLAB function inverse FFT (IFFT) was used for IDFT computation.

3) *Sum-of-Sinusoids*: The method used was the WSS-improved Jakes' model of [7]. Following this model, the normalized low-pass discrete fading process is generated by

$$x[n] = x_c[n] + jx_s[n] \quad (19a)$$

$$x_c[n] = \frac{1}{\sqrt{N_s}} \sum_{k=1}^{N_s} \cos(2\pi f_m n \cos \alpha_k + \phi_k) \quad (19b)$$

$$x_s[n] = \frac{1}{\sqrt{N_s}} \sum_{k=1}^{N_s} \cos(2\pi f_m n \sin \alpha_k + \varphi_k) \quad (19c)$$

with

$$\alpha_k = \frac{2\pi k - \pi + \theta}{4N_s}, \quad k = 1, 2, \dots, N_s \quad (20)$$

where ϕ_k , φ_k and θ are statistically independent and uniformly distributed on $[-\pi, \pi)$ for all k . The statistical properties of $x[n]$ asymptotically approach those of Clarke's isotropic model as the number of sinusoids approaches infinity, while very good approximation to the ensemble statistics has been reported when N_s is not less than 8 [7]. For finite N_s , it is important to point out that this WSS simulator is not autocorrelation ergodic. That is, the infinite time-average autocorrelation is a random variable and unlike the IDFT and AR simulators, the statistical information contained in each output waveform or sample function is not identical and may deviate from the desired statistics of the theoretical model [35].

C. Performance Comparisons

The quality measures described in [40] were used to compare the AR variate generation method to the modified IDFT technique of [2] and to the WSS sinusoidal generator of [7]. The results, which are presented in Table I, compare the quality of the real part of the simulator outputs. Similar results were achieved for the imaginary sequences and these are omitted for brevity. Perfect variate generation corresponds to 0 dB for both measures. In all cases, the reference ACF is (2) with a normalized maximum Doppler of $f_m = 0.05$. A bias of $\epsilon = 10^{-8}$ was used to condition the Yule-Walker equations for all AR model orders. An autocorrelation sequence length of 200 was considered for evaluation of (17) and (18). The theoretical (T) results for the IDFT routine were computed as proposed in [2] for the IDFT routine, and using (9) and (14) for the AR generator. For the empirical (E) results, time-average correlations were calculated based on 2^{20} generated samples. The computed quality measures were then averaged over 50 independent simulation trials. Plots of the empirical correlations of the IDFT and AR generator outputs are shown in Fig. 4. The empirical correlations for a typical simulation

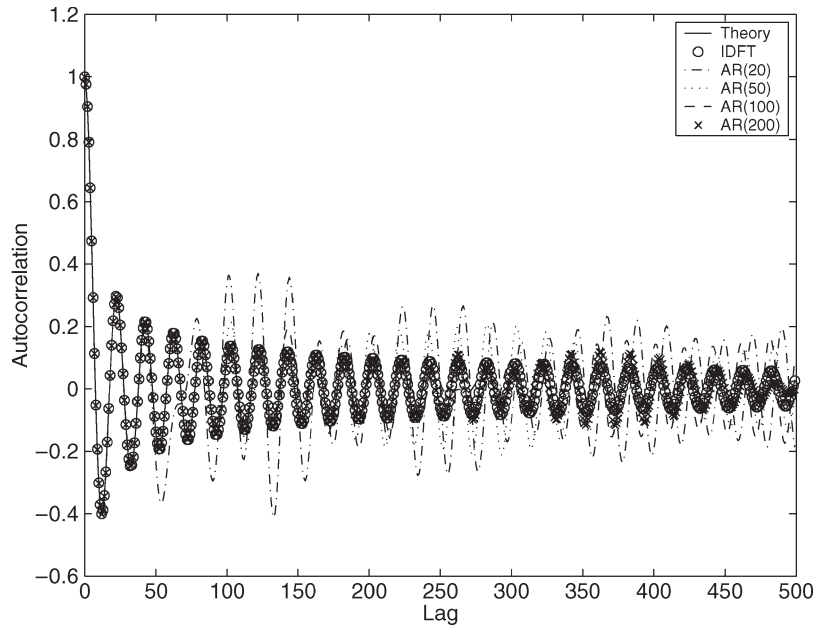


Fig. 4. Empirical autocorrelations for the AR and IDFT methods.

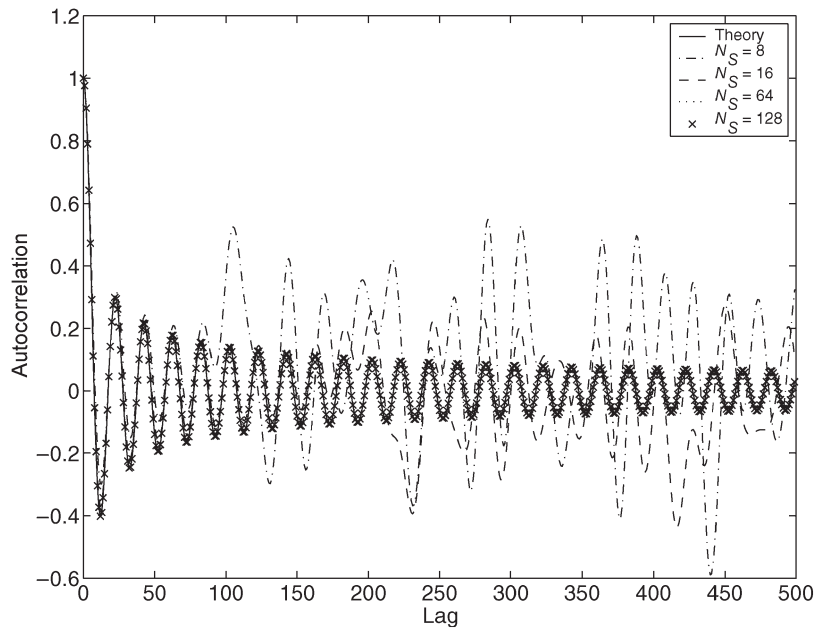


Fig. 5. Empirical time-average autocorrelations for the sum-of-sinusoids method.

run of the nonergodic WSS sinusoidal generator are provided in Fig. 5.

The results demonstrate that the IDFT technique, whose theoretical accuracy is only limited by small aliasing errors [41], generally provides closer ACF matching over a wider range of lags. However, the correlation matching property of the AR method allows it to provide a more precise match to the desired ACF over the order of the model used. Similar accuracy can be achieved by the sinusoidal generator when a large number of sinusoids is used. The mild benefits of this tradeoff on the variate quality can be observed by comparing the generator outputs with regards to other important statistics. For

example, in Fig. 6, the normalized level-crossing rate, defined as the rate at which the envelope crosses a specified level in the positive direction, is computed for the IDFT, AR(50), and $N_s = 64$ sinusoidal generator outputs and compared with the theoretical value given by [17, eq. (1.3–37)]. Since the LCR statistic depends strongly on the first two moments of the Doppler spectrum, or equivalently, the curvature of the ACF at the zeroth lag [17], the AR simulator provides an excellent match by virtue of its correlation matching property, better than the match achieved with the IDFT method. A comparable match is achieved using the WSS sinusoidal generator, but only when a large number of sinusoids is used. We report that

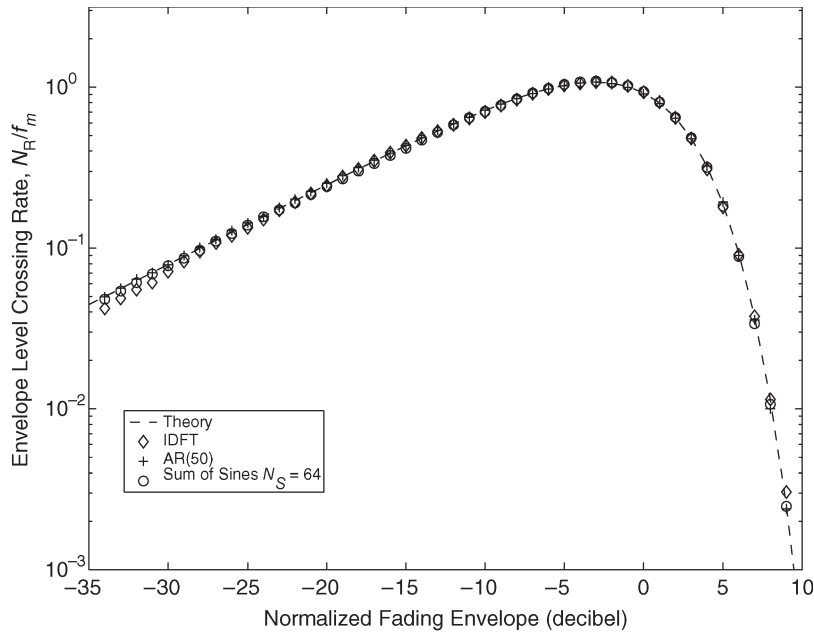


Fig. 6. Empirical level-crossing rates for the AR(50), IDFT, and $N_s = 64$ sum-of-sinusoids simulators.

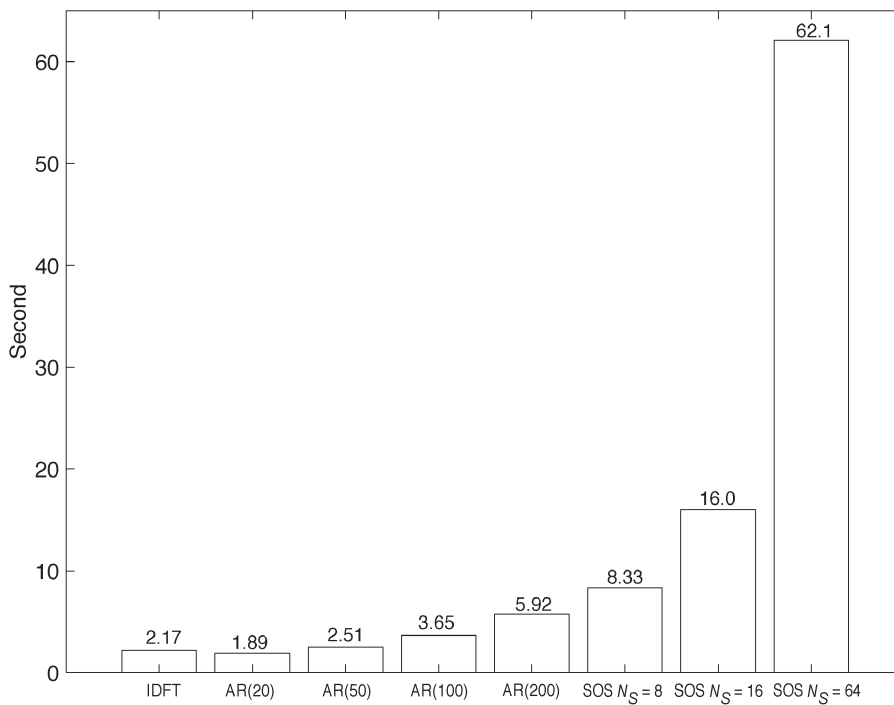


Fig. 7. The time to generate 2^{21} complex samples using the various generation methods.

to generate the level-crossing rate curves, 2^{20} variates with a normalized Doppler of $f_m = 0.001$ were used.

To assess the relative computational effort required to generate variates using the AR, IDFT, and WSS sum-of-sinusoids methods, sequences of length 2^{21} were generated on a Pentium IV machine using routines coded in MATLAB. The sequence length was chosen as a power of two as this is favorable for the IDFT method [2]. The reference ACF was (2) with $f_m = 0.05$. Results for the time comparisons are

presented in Fig. 7. The IDFT method, owing to the inherent efficiency of the FFT operation, is superior in this regard. With the sinusoidal generator of [7], a large effort is required to ensure that the quadrature components of each generated sample function have accurate correlation statistics. Almost 30 times more time than the IDFT method was needed to generate the variates using the accurate $N_s = 64$ simulator. As for the AR approach, it can only be performed faster than the IDFT method for short IIR filter lengths, with a

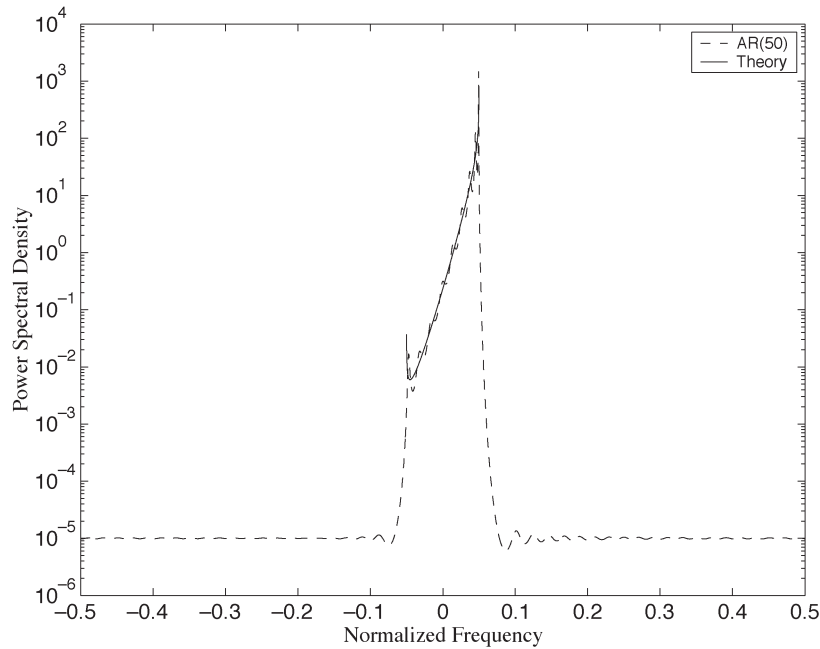


Fig. 8. The power spectral density of the nonisotropic model with $f_m = 0.05$, $\kappa = 5$, $\mu = 0$, and the corresponding complex AR(50) model fit with $\epsilon = 10^{-5}$.

corresponding loss in modeling accuracy. Almost three times more time was needed to compute the model coefficients and generate the variates using a highly accurate AR(200) model. However, the AR method can be considered efficient when compared to the required effort of the sinusoidal generator. In practical applications, it is likely that theoretically predicted differences less than 0.2 dB will be vitiated by implementation tolerances or limits to the theoretical models. From this point of view, the AR(50) model may be comparable to the IDFT method. Fig. 7 shows that the AR(50) model requires only 1.2 times more time than the IDFT method. The main advantage of the AR filtering and WSS sinusoidal methods is that fading variates can be generated as they are required. In contrast, the computational efficiency of the IDFT approach comes at a cost in storage requirements as all variates are generated using a single IFFT. Thus, for very long sequence lengths, the IDFT implementation may require unavailable memory. The AR and sinusoidal generators, however, do not have such a limitation. One disadvantage of the AR approach is that the model coefficients need to be recomputed when f_m is changed. For the WSS sinusoidal method, one does not have to recalculate any coefficients.

To reduce the computational load of the AR simulator, a multirate filtering implementation is recommended [5], [42]. With this approach, the spectrum shaping filter is cascaded with an interpolator. This allows for the generation of the complex channel gain at a low sampling rate, typically a few multiples of the Doppler frequency, with correspondingly shorter AR shaping filters. A comparatively simple FIR interpolator (e.g., MMSE, raised cosine, etc.) can then accurately provide the necessary rate conversion to the desired sampling rate. When combined with the addition of a small constant as described in Section III, interpolation proves useful in mitigating numerical problems that occur when fitting an

AR model to a very-small-bandwidth Doppler spectrum. Based on our simulations, interpolation is suggested for the simulation of channels with normalized Doppler rates on the order of $f_m = 0.001$ or smaller.

D. Nonisotropic Fading Simulation

In this subsection, we examine the use of the AR method for accurately synthesizing nonisotropic Rayleigh fading channels. For directional scenarios, the nonuniform probability density function for the angle of arrival (AOA) at the receiver can result in a baseband Doppler PSD which is not symmetric around the $f = 0$ frequency or, correspondingly, a channel ACF, which is complex valued. The underlying real in-phase and quadrature Gaussian processes are cross-correlated in such cases. Such Rayleigh processes can be well approximated using a complex AR process and following the methodology in Section III. The complex AR coefficients are determined using the complex form of the Levinson–Durbin algorithm in this case. As an example, a plausible model for the directional AOA, which conveniently results in closed-form correlation and Doppler PSD functions, is the parametric Von Mises/Tikhonov distribution function [22]

$$p(\theta) = \frac{\exp[\kappa \cos(\theta - \mu)]}{2\pi I_0(\kappa)}, \quad \theta \in [-\pi, \pi] \quad (21)$$

where $I_0(\cdot)$ is the zeroth order modified Bessel function [43], μ represents the mean direction of the AOA, and κ controls the beamwidth. This model, which includes the uniform AOA distribution as a special case ($\kappa = 0$), was corroborated with some empirical measurements of narrowband fading channels in [22]. For the AOA distribution in (21), the corresponding

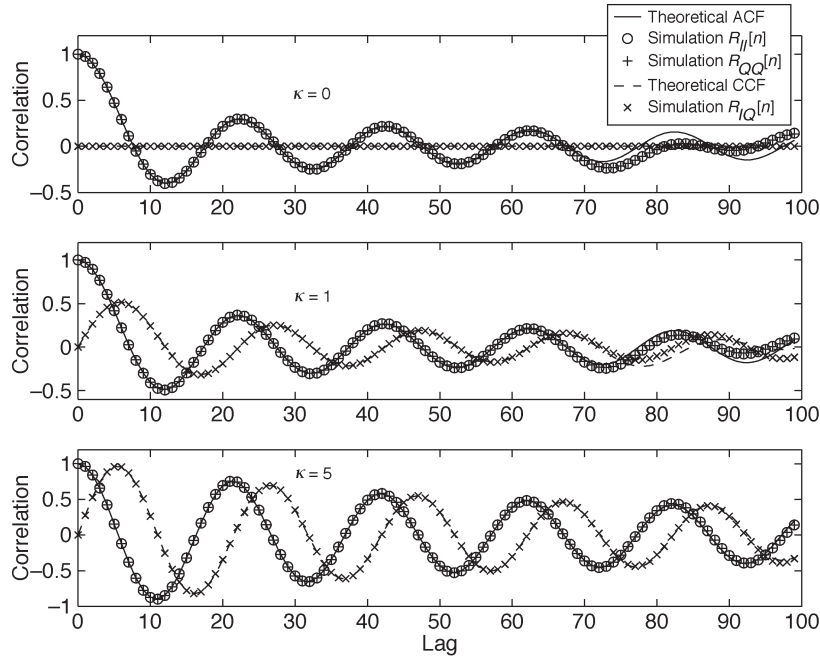


Fig. 9. The empirical autocorrelation and I/Q cross-correlations corresponding to the nonisotropic simulation examples.

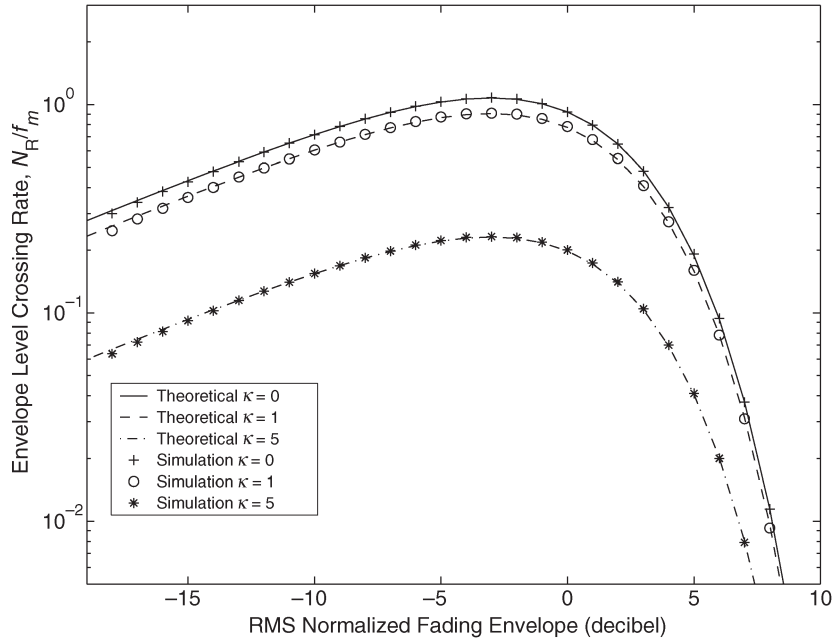


Fig. 10. The empirical level-crossing rates corresponding to the nonisotropic simulation examples.

sampled autocorrelation of the Rayleigh fading channel can be shown to be [22]

$$R[n] = R_{II}[n] + jR_{IQ}[n]$$

$$= \frac{I_0 \left(\sqrt{\kappa^2 - (2\pi f_m |n|)^2} + 4j\kappa \cos(\mu)\pi f_m |n| \right)}{I_0(\kappa)} \quad (22)$$

where $R_{II}[n] = R_{QQ}[n]$, $R_{II}[n]$, and $R_{QQ}[n]$ denote the sampled autocorrelation of the real in-phase and quadrature Gaussian processes, respectively and $R_{IQ}[n]$ denotes the cross-correlation function. The corresponding PSD is given by [22, eq. (3)]. Accurate simulation of such nonisotropic Rayleigh models can be easily accomplished using a complex AR model. For example, a complex AR(50) model was used to synthesize fading processes with $f_m = 0.05$ and $\mu = 0$ for scenarios with $\kappa = 0$ (isotropic), $\kappa = 1$ (slightly nonisotropic), and $\kappa = 5$ (highly nonisotropic). In each case, a bias of $\epsilon = 10^{-5}$ was

used to condition the inputs to the complex Levinson recursion. The PSD of the nonisotropic model and the AR(50) approximation are shown in Fig. 8 for the directional $\kappa = 5$ case. The empirical autocorrelations and I/Q cross-correlations are plotted in Fig. 9 and these are found to provide a very accurate approximation of the desired statistics. The empirical normalized level crossing rates are shown in Fig. 10 and compared to the values in [44, eq. (19)]. The excellent agreement seen in these results serves to verify the theoretical nonisotropic Rayleigh LCR expression derived in [44].

V. CONCLUSION

Autoregressive (AR) stochastic models were considered for the computer simulation of correlated Rayleigh fading channels. The numerical difficulties faced by this approach were resolved by approximating the deterministic bandlimited Doppler processes with regular processes. Two procedures for eliminating the need to discard, possibly many, initial generated samples due to transient distortion were presented. The proposed methods enable the synthesis of stationary and statistically accurate Rayleigh channel gain samples as they are needed. Furthermore, the fading channel ACF is easily specified, which makes the simulator especially suited for the emulation of generalized flat Rayleigh fading channels. To demonstrate the general applicability of the method, an AR simulator for generating nonisotropic fading channel variates was derived. This nonisotropic simulator will be useful for emulating directional fading scenarios encountered in practical mobile communication systems.

ACKNOWLEDGMENT

The authors wish to thank D. J. Young of the iCORE Wireless Communications Laboratory at the University of Alberta for providing the MATLAB implementation of the IDFT algorithm of [2].

REFERENCES

- [1] R. H. Clarke, "A statistical theory of mobile-radio reception," *Bell Syst. Tech. J.*, vol. 47, no. 6, pp. 957–1000, Jul.–Aug. 1968.
- [2] D. J. Young and N. C. Beaulieu, "The generation of correlated Rayleigh random variates by inverse Fourier transform," *IEEE Trans. Commun.*, vol. 48, no. 7, pp. 1114–1127, Jul. 2000.
- [3] C. Loo and N. Secord, "Computer models for fading channels with applications to digital transmission," *IEEE Trans. Veh. Technol.*, vol. 40, no. 4, pp. 700–707, Nov. 1991.
- [4] P. Höher, "A statistical discrete-time model for the WSSUS multipath channel," *IEEE Trans. Veh. Technol.*, vol. 41, no. 4, pp. 461–468, Jul. 1992.
- [5] D. Verdin and T. Tozer, "Generating a fading process for the simulation of land-mobile radio communications," *Electron. Lett.*, vol. 29, no. 23, pp. 2011–2012, Nov. 11, 1993.
- [6] M. F. Pop and N. C. Beaulieu, "Limitations of sum-of-sinusoids fading channel simulators," *IEEE Trans. Commun.*, vol. 49, no. 4, pp. 699–708, Apr. 2001.
- [7] Y. R. Zheng and C. Xiao, "Improved models for the generation of multiple uncorrelated Rayleigh fading waveforms," *IEEE Commun. Lett.*, vol. 6, no. 6, pp. 256–258, Jun. 2002.
- [8] —, "Simulation models with correct statistical properties for Rayleigh fading channels," *IEEE Trans. Commun.*, vol. 51, no. 6, pp. 920–928, Jun. 2003.
- [9] M. Tsatsanis and Z. Xu, "Pilot symbol assisted modulation in frequency selective fading wireless channels," *IEEE Trans. Signal Process.*, vol. 48, no. 8, pp. 2353–2365, Aug. 2000.
- [10] H. Wu and A. Duel-Hallen, "Multiuser detectors with disjoint Kalman channel estimators for synchronous CDMA mobile radio channels," *IEEE Trans. Commun.*, vol. 48, no. 5, pp. 752–756, May 2000.
- [11] Y. Ara and H. Ogiwara, "Adaptive equalization of selective fading channel based on AR-model of channel impulse response fluctuation," *Electron. Commun. Jpn.*, pt. 1, vol. 74, no. 7, pp. 76–86, 1991.
- [12] V. Kafedziski and D. Morrell, "Optimal adaptive equalization of multipath fading channels," in *Proc. IEEE Asilomar Conf. Signals, Systems, and Computers*, Pacific Grove, CA, 1994, pp. 1443–1447.
- [13] T. Eyceoz, A. Duel-Hallen, and H. Hallen, "Deterministic channel modeling and long range prediction of fast fading mobile radio channels," *IEEE Commun. Lett.*, vol. 2, no. 9, pp. 254–256, Sep. 1998.
- [14] Q. T. Zhang, "A decomposition technique for efficient generation of correlated Nakagami fading channels," *IEEE J. Sel. Areas Commun.*, vol. 18, no. 11, pp. 2385–2392, Nov. 2000.
- [15] G. Colman, S. Blostein, and N. C. Beaulieu, "An ARMA multipath fading simulator," in *Wireless Personal Communications: Improving Capacity, Services and Reliability*. Boston, MA: Kluwer, 1997.
- [16] P. A. Bello, "Characterization of randomly time-variant linear channels," *IEEE Trans. Commun. Syst.*, vol. CS-11, no. 4, pp. 360–393, Dec. 1963.
- [17] W. C. Jakes, *Microwave Mobile Communications*. New York: Wiley, 1974.
- [18] T. Aulin, "A modified model for the fading signal at a mobile radio channel," *IEEE Trans. Veh. Technol.*, vol. 28, no. 3, pp. 182–203, Feb. 1979.
- [19] J. D. Parsons and A. D. Turkmani, "Characterisation of mobile radio signals: Model description," *Proc. Inst. Elect. Eng.*, pt. 1, vol. 138, no. 6, pp. 549–555, Apr. 1991.
- [20] R. H. Clarke and W. L. Khoo, "3-D mobile radio channel statistics," *IEEE Trans. Veh. Technol.*, vol. 46, no. 3, pp. 798–799, May 1997.
- [21] J. Sadowsky and V. Kafedziski, "On the correlation and scattering functions of the WSSUS channel for mobile communications," *IEEE Trans. Veh. Technol.*, vol. 47, no. 1, pp. 270–282, Feb. 1998.
- [22] A. Abdi, J. Barger, and M. Kaveh, "A parametric model for the distribution of the angle of arrival and the associated correlation function and power spectrum at the mobile station," *IEEE Trans. Veh. Technol.*, vol. 51, no. 1, pp. 425–434, May 2002.
- [23] A. Leon-Garcia, *Probability and Random Processes for Electrical Engineering*. Reading, MA: Addison-Wesley, 1990.
- [24] J. I. Smith, "A computer generated multipath fading simulation for mobile radio," *IEEE Trans. Veh. Technol.*, vol. VT-24, no. 3, pp. 39–40, Aug. 1975.
- [25] S. M. Kay, *Modern Spectral Estimation*. Englewood Cliffs, NJ: Prentice-Hall, 1988.
- [26] A. Giordano and F. Hsu, *Least Square Estimation with Applications to Digital Signal Processing*. New York: Wiley, 1985.
- [27] S. Haykin, *Adaptive Filter Theory*, 2nd ed. Englewood Cliffs, NJ: Prentice-Hall, 1991.
- [28] A. Papoulis, *Probability, Random Variables, and Stochastic Processes*. New York: McGraw-Hill, 1991.
- [29] —, "Predictable processes and Wold's decomposition: A review," *IEEE Trans. Acoust. Speech Signal Process.*, vol. ASSP-33, no. 4, pp. 933–938, Aug. 1985.
- [30] R. J. Lyman, W. W. Edmonson, S. McCullough, and M. Rao, "The predictability of continuous-time, bandlimited processes," *IEEE Trans. Signal Process.*, vol. 48, no. 2, pp. 311–316, Feb. 2000.
- [31] R. J. Lyman, "Optimal mean-square prediction of the mobile-radio fading envelope," *IEEE Trans. Signal Process.*, vol. 51, no. 3, pp. 819–824, Mar. 2003.
- [32] B. Picinbono and J. Kerilis, "Some properties of prediction and interpolation errors," *IEEE Trans. Acoust. Speech Signal Process.*, vol. 36, no. 4, pp. 525–531, Apr. 1988.
- [33] D. Slepian, "Prolate spheroidal wave functions, Fourier analysis, and uncertainty—V: The discrete case," *Bell Syst. Tech. J.*, vol. 57, no. 5, pp. 1371–1430, May 1978.
- [34] M. Rosenblatt, "Some purely deterministic processes," *J. Math. Mech.*, vol. 6, no. 6, pp. 801–810, Nov. 1957.
- [35] K. E. Baddour, "Simulation, estimation and prediction of flat fading wireless channels," Ph.D. dissertation, Dept. Elect. Comput. Eng., Queens Univ., Kingston, ON, Canada.
- [36] D. G. Lampard, "The response of linear networks to suddenly applied random noise," *IRE Trans. Circuit Theory*, vol. CT-2, pp. 49–57, Mar. 1955.
- [37] J. R. M. Hosking, "Some models of persistence in time series," in *Time*

Series Analysis: Theory and Practice I, O. D. Anderson, Ed. Amsterdam, The Netherlands: North Holland, 1982, pp. 641–653.

- [38] F. L. Ramsey, "Characterization of the partial autocorrelation function," *Ann. Stat.*, vol. 6, no. 6, pp. 1296–1301, 1974.
- [39] B. Friedlander, "Lattice filters for adaptive processing," *Proc. IEEE*, vol. 70, no. 8, pp. 829–867, Aug. 1982.
- [40] D. J. Young and N. C. Beaulieu, "Power margin quality measures for correlated random variates derived from the normal distribution," *IEEE Trans. Inf. Theory*, vol. 49, no. 1, pp. 241–252, Jan. 2003.
- [41] N. C. Beaulieu and C. C. Tan, "FFT based generation of band-limited Gaussian noise variates," *Eur. Trans. Telecommun.*, vol. 10, no. 1, pp. 540–550, Sep./Oct. 1999.
- [42] H. Brehm, W. Stammner, and M. Woerner, "Design of a highly flexible digital simulator for narrowband fading channels," in *Signal Processing III: Theories and Applications, EURASIP*. North Holland, The Netherlands: Elsevier, 1986, pp. 1113–1116.
- [43] M. Abramowitz and I. Stegun, *Handbook of Mathematical Functions*. New York: Dover, 1965.
- [44] A. Abdi, K. Wills, H. Barger, S. Alouini, and M. Kaveh, "Comparison of level crossing rate and average fade duration of Rayleigh, Rice, and Nakagami fading models with mobile channel data," in *Proc. IEEE Vehicular Technology Conf.*, Boston, MA, 2000, pp. 1850–1857.



Kareem E. Baddour (S'93) received the B.Eng. degree in electrical engineering in 1996 from Memorial University of Newfoundland, St. John's, NF, Canada, and the M.Sc. (Eng.) degree in 1998 from Queen's University, Kingston, ON, Canada, where he is currently working towards the Ph.D. degree in the Department of Electrical and Computer Engineering.

Previously, he was with Northern Telecom, Newbridge Networks, Microtel Pacific Research, as well as with the Canadian Coast Guard's Telecommunications and Electronics Branch. He is also affiliated

with the iCORE Wireless Communications Laboratory at the University of Alberta, Edmonton, AB, Canada. His current research interests lie in the general area of wireless communications, with a focus on fading channel simulation, estimation, prediction, and equalization.

Mr. Baddour has received numerous scholarships, including two Natural Sciences and Engineering Research Council of Canada (NSERC) Postgraduate Scholarships, two Industry Canada Fessenden Postgraduate Scholarships, and an Ontario Graduate Scholarship in Science and Technology. He received the Memorial University Medal for Electrical Engineering in 1996.



Norman C. Beaulieu (S'82–M'86–SM'89–F'99) received the B.A.Sc. (honors), M.A.Sc., and Ph.D. degrees in electrical engineering from the University of British Columbia, Vancouver, Canada, in 1980, 1983, and 1986, respectively.

He was a Queen's National Scholar Assistant Professor from September 1986 to June 1988, an Associate Professor from July 1998 to June 1993, and a Professor from July 1993 to August 2000 with the Department of Electrical Engineering, Queen's University, Kingston, ON, Canada. In September 2000,

he became the iCORE Research Chair in Broadband Wireless Communications at the University of Alberta, Edmonton, Canada, and, in January 2001, he became the Canada Research Chair in Broadband Wireless Communications. His current research interests include broadband digital communications systems, fading channel modeling and simulation, interference prediction and cancellation, decision-feedback equalization, and space-time coding.

Dr. Beaulieu is a Member of the IEEE Communication Theory Committee and served as its Representative to the Technical Program Committee for the 1991 International Conference on Communication and as Co-Representative to the Technical Program Committee for the 1993 International Conference on Communications and the 1996 International Conference on Communications. He was General Chair of the Sixth Communication Theory Mini-Conference in association with GLOBECOM'97 and Co-Chair of the Canadian Workshop on Information Theory 1999. He has been an Editor of the IEEE TRANSACTIONS ON COMMUNICATIONS for wireless communication theory since January 1992 and has served on the Editorial Board of the PROCEEDINGS OF THE IEEE since November 2000. He served as Editor-in-Chief of the IEEE TRANSACTIONS ON COMMUNICATIONS from January 2000 to December 2003 and as an Associate Editor of the IEEE COMMUNICATIONS LETTERS for wireless communication theory from November 1996 to August 2003. He received the Natural Science and Engineering Research Council of Canada (NSERC) E. W. R. Steacie Memorial Fellowship in 1999. He was awarded the University of British Columbia Special University Prize in Applied Science in 1980 as the highest standing graduate in the Faculty of Applied Science. He is a Fellow of The Royal Society of Canada.